

AD-A062 828

AEROSPACE CORP EL SEGUNDO CALIF IVAN A GETTING LABS  
SCATTERING OF SOLAR RADIATION BY CLOUDS. (U)

F/G 20/6

DEC 78 S J YOUNG

F04701-78-C-0079

UNCLASSIFIED

TR-0079(4970-40)-1

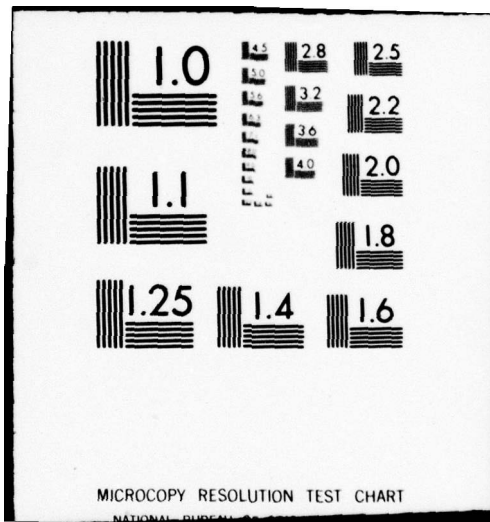
SAMSO-TR-78-178

NL

1 OF  
AD  
A062 828



END  
DATE  
FILED  
2-79  
DDC



REPORT SAMSO-TR-78-17B

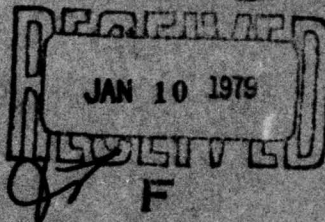
LEVEL

(12)  
F

AD A062828

## Scattering of Solar Radiation by Clouds

DDC



S. J. YOUNG  
/ Chemistry and Physics Laboratory/  
The Ivan A. Getting Laboratories  
The Aerospace Corporation  
El Segundo, Calif. 90245

5 December 1978

Interim Report

APPROVED FOR PUBLIC RELEASE;  
DISTRIBUTION UNLIMITED

79 01 09 044

Prepared for

SPACE AND MISSILE SYSTEMS ORGANIZATION  
AIR FORCE SYSTEMS COMMAND  
Los Angeles Air Force Station  
P.O. Box 92960, Worldwide Postal Center  
Los Angeles, Calif. 90009

This interim report was submitted by The Aerospace Corporation, El Segundo, CA 90245, under Contract No. F04701-78-C-0079 with the Space and Missile Systems Organization, Contracts Management Office, P.O. Box 92960, Worldway Postal Center, Los Angeles, CA 90009. It was reviewed and approved for The Aerospace Corporation by S. Siegel, Director, Chemistry and Physics Laboratory. Gerhard E. Aichinger was the project officer for Mission-Oriented Investigation and Experimentation (MOIE) Programs.

This report has been reviewed by the Information Office (OI) and is releasable to the National Technical Information Service (NTIS). At NTIS, it will be available to the general public, including foreign nations.

This technical report has been reviewed and is approved for publication. Publication of this report does not constitute Air Force approval of the report's findings or conclusions. It is published only for the exchange and stimulation of ideas.



Gerhard E. Aichinger  
Project Officer

FOR THE COMMANDER

Frank J. Bane, Chief  
Contracts Management Office

## UNCLASSIFIED

SECURITY CLASSIFICATION OF THIS PAGE (When Data Entered)

19 REPORT DOCUMENTATION PAGE		READ INSTRUCTIONS BEFORE COMPLETING FORM
1. REPORT NUMBER SAMSO TR-78-178	2. GOVT ACCESSION NO.	3. RECIPIENT'S CATALOG NUMBER
4. TITLE (and Subtitle) SCATTERING OF SOLAR RADIATION BY CLOUDS		5. TYPE OF REPORT & PERIOD COVERED Interim <i>rept.</i>
6. AUTHOR(s) Stephen J. Young		7. PERFORMING ORG. REPORT NUMBER TR-0079(4970-40)-1
8. AUTHOR(s) Stephen J. Young		9. CONTRACT OR GRANT NUMBER(s) F04701-78-C-0079
10. PERFORMING ORGANIZATION NAME AND ADDRESS The Aerospace Corporation El Segundo, Calif. 90245		11. PROGRAM ELEMENT, PROJECT, TASK AREA & WORK UNIT NUMBERS <i>12 48P.</i>
11. CONTROLLING OFFICE NAME AND ADDRESS Space and Missile Systems Organization Air Force Systems Command Los Angeles, Calif. 90009		12. REPORT DATE 5 Dec 1978
13. NUMBER OF PAGES 48		14. SECURITY CLASS. (of this report) Unclassified
15. DECLASSIFICATION/DOWNGRADING SCHEDULE		
16. DISTRIBUTION STATEMENT (of this Report)  Approved for public release; distribution unlimited		
17. DISTRIBUTION STATEMENT (of the abstract entered in Block 20, if different from Report)		
18. SUPPLEMENTARY NOTES		
19. KEY WORDS (Continue on reverse side if necessary and identify by block number) Cloud Reflectance Cloud Scattering Solar Reflection Solar Scattering		
20. ABSTRACT (Continue on reverse side if necessary and identify by block number) Several simple models for computing the diffuse reflectance of solar radiation from plane-parallel cloud layers are formulated and assessed for accuracy. None of the models in their simplest form is suitable for application within the constraint of a factor of two accuracy. However, an empirical modification of the single-scattering model yields a procedure for computing the diffuse reflection coefficient with a nominal error of <50 percent.		

DD FORM 1473 A  
(FACSIMILE)

79 01 09 044

UNCLASSIFIED 409 944  
*mt*

SECURITY CLASSIFICATION OF THIS PAGE (When Data Entered)

## CONTENTS

1. INTRODUCTION.....	7
2. EQUATION OF RADIATIVE TRANSFER.....	9
3. TEST CONDITIONS.....	13
4. MODEL DESCRIPTIONS AND RESULTS.....	23
A. Single-Scattering Model.....	23
B. Two-Stream Theoretical Modification of the Single-Scattering Model .....	25
C. Empirical Modification of the Single- Scattering Model .....	30
D. Turner Approximation.....	33
E. Romanova Approximation.....	37
F. Truncation Approximation .....	40
G. Expansion in Orders of Scattering.....	43
5. SUMMARY .....	47
REFERENCES.....	49

ACCESSION for	
NTIS	White Section <input checked="" type="checkbox"/>
DDC	Buff Section <input type="checkbox"/>
UNCLASSIFIED	
JUL 1968	
DISSEMINATION BY REFERENCES	
SPECIAL	
<i>[Handwritten signature]</i>	

## FIGURES

1. Coordinate System for Radiative Transfer in a Plane-Parallel Cloud Layer .....	10
2. Particle Size Distribution for Model Cumulus Cloud .....	14
3. Index of Refraction of Water .....	15
4. Total Cross Sections for Model Cumulus Cloud .....	16
5. Differential Scattering Cross Section for Model Cumulus Cloud .....	17
6. Forward Scattering Parameter for Model Cumulus Cloud .....	19
7. Single Particle Scattering Albedo for Model Cumulus Cloud .....	20
8. Test Standard Cloud Reflectance .....	21
9. Comparison of Single-Scattering Approximations with Test Case .....	24
10. Comparison between Single-Scattering Model and Experimental Data in the $2.7\text{-}\mu\text{m}$ Spectral Region .....	26
11. Correction Factors for the Modified Single-Scattering Models .....	32
12. Predicted Cloud Reflectance with Single-Scattering and Modified Single-Scattering Models .....	34
13. Comparison of Turner Model Prediction with Test Case .....	36
14. Comparison of Romanova-Isotropic Model Prediction with Test Case .....	41

## TABLES

1. Data for Construction of Empirically Modified Single-Scattering Model .....	31
2. Summary of Reflectance Models .....	48

## 1. INTRODUCTION

Infrared radiation from clouds is an important background signal contribution that must be considered in the design of high-altitude sensor systems deployed for missile and aircraft detection. Thermal radiation from clouds and its transmittance through the atmosphere can be computed in a relatively straightforward manner. On the other hand, the calculation of apparent cloud radiance that results from the diffuse reflection of solar radiation from clouds is a much more complicated problem in multiple-scattering radiative transfer theory. Even with the simplifying assumptions of an infinite, plane-parallel cloud layer composed of spherical particles, the computation of exact solutions of the reflected radiation field for arbitrary solar and viewing angles is complex and time consuming, prohibitively so for routine application to parametric system design studies. The overall objective of the present study is to investigate approximate cloud reflectance models that can be effectively applied in systems analysis.

The accuracy of these models is not of paramount importance. The problem is usually phrased by the system analyst as "how much reflectance would I expect from high-altitude clouds" without any specification of cloud type, homogeneity of cloud cover, particle type or size distribution, etc. At the same time, very large errors cannot be acceptable since these could presumably influence the system design. The subjective criterion set for acceptable model accuracy here is that the model should predict within a factor of two of the exact reflectance for a typical cloud type. The cloud type chosen is a model, plane-parallel, semi-infinite cumulus cloud composed of spherical water or ice particles. Further consideration of this test standard is made in Section 3.

The method of approach to the problem is straightforward. A literature search was made for suitable models that appeared amenable to the problem. The methods were adapted to the present problem in the simplest manner possible and the predictions for the test standard compared to the exact results for the standard case.

## 2. EQUATION OF RADIATIVE TRANSFER

Consider parallel solar radiation of spectral flux density  $E_0$  (W/cm<sup>2</sup> -  $\mu\text{m}$ ) impinging on the top of a plane-parallel, homogeneous cloud layer at zenith angle  $\theta_0$  (see Fig. 1).<sup>(1, 2, 3)</sup> The incoming radiation is scattered by the particles comprising the cloud, and a steady state spectral radiance field  $L(\tau, \mu, \phi)$  (W/cm<sup>2</sup> - sr -  $\mu\text{m}$ ) is established within the cloud.  $\tau$  is a dimensionless measure of distance into the cloud (from the top) and is defined later.  $\mu$  is the zenith angle variable  $\mu = \cos\theta$ . The field  $L$  is composed of two parts, a direct component  $L_0$  which contributes to  $L$  only for  $\theta = \pi - \theta_0$  and  $\phi = \phi_0$ , and a diffuse component  $L_D$ . The solution for the direct component is  $L_0 = E_0 \exp(-\mu\tau)$ . The diffuse component for a plane-parallel, vertically homogeneous cloud of infinite horizontal extent under conditions of thermodynamic equilibrium and with no embedded sources of radiation is governed by the following integro-differential equation of radiative transfer:

$$\mu \frac{dL(\tau, \mu, \phi)}{d\tau} = L(\tau, \mu, \phi) - \frac{1}{4\pi} \int_0^{2\pi} \int_{-1}^1 p(\mu, \phi, \mu', \phi') L(\tau, \mu', \phi') d\mu' d\phi' - \frac{1}{4\pi} E_0 e^{-\tau/\mu_0} p(\mu, \phi, -\mu_0, \phi_0). \quad (1)$$

Note that the subscript D has been dropped. From this point on, the symbol L will be used to denote  $L_D$ . The function  $p(\mu, \phi, \mu', \phi')$  is the scattering phase function for the cloud particles and describes the probability for scattering by a single particle from the direction  $\mu'\phi'$  to the direction  $\mu\phi$ . For spherical particles,  $p$  does not depend individually on  $\mu$  and  $\phi$  but is a function only of the scattering angle  $\varphi$  defined by

$$\cos\varphi = \cos(\phi - \phi') \sqrt{(1 - \mu^2)(1 - \mu'^2) + \mu\mu'}. \quad (2)$$

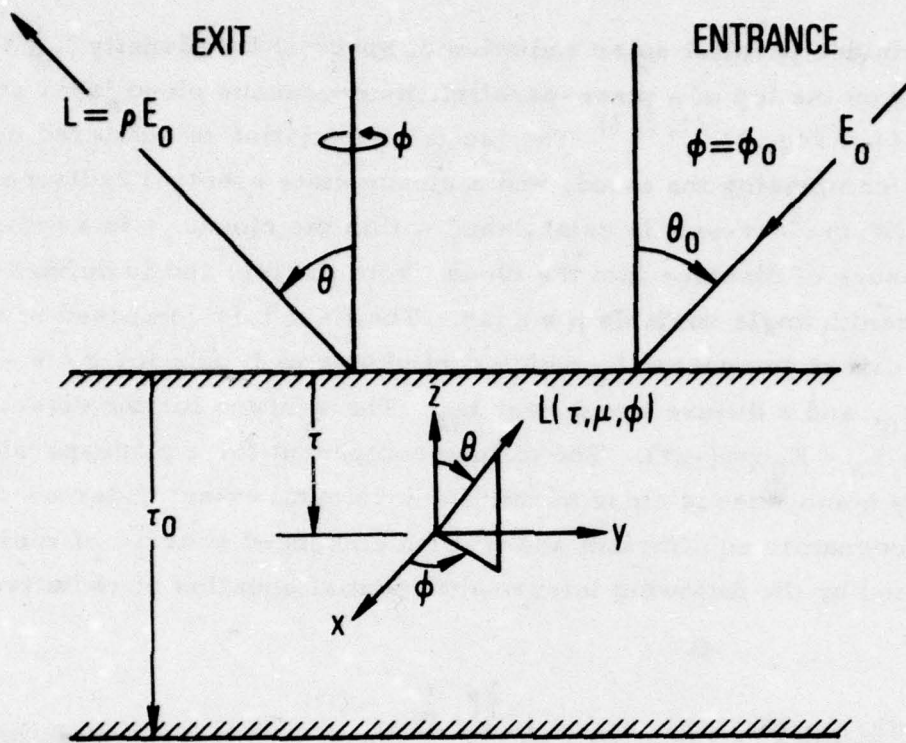


Fig. 1. Coordinate System for Radiative Transfer in a Plane-Parallel Cloud Layer

The phase function is normalized such that

$$\int_0^{2\pi} \int_{-1}^1 p(\mu, \phi, \mu', \phi') d\mu' d\phi' = 2\pi \int_{-1}^1 p(x) dx = 4\pi \omega_0. \quad (3)$$

where  $x = \cos\phi$ .  $\omega_0$  is the single-scattering albedo of the cloud particles and is defined in terms of the particle cross sections for absorption ( $\sigma_a$ ) and scattering ( $\sigma_s$ ) by

$$\omega_0 = \frac{\sigma_s}{\sigma_e} \quad (4)$$

where  $\sigma_e$  is the total extinction cross section  $\sigma_e = \sigma_s + \sigma_a$ . These cross sections, and the differential scattering cross section  $d\sigma_s(\phi)/d\Omega$  which defines the phase function through

$$p(\cos\phi) = \frac{4\pi}{\sigma_e} \frac{d\sigma_s(\phi)}{d\Omega} \quad (5)$$

are considered in the following section. The optical depth parameter  $\tau$  is defined by  $\tau = N\sigma_e z$  where  $N$  is the cloud particle density.

The boundary conditions that the radiance field  $L$  must satisfy are (1) that there be no downward directed diffuse radiance at the top of the cloud, i. e.,

$$L(0, \mu, \phi) = 0 \quad \mu < 0, \quad (6)$$

and (2) for a finite thickness cloud, that there be no upward directed radiance at the bottom, i. e.,

$$L(\tau_0, \mu, \phi) = 0 \quad \mu > 0, \quad (7)$$

or (3), for a semi-infinite cloud, that  $L(\tau)$  remain bounded as  $\tau \rightarrow \infty$ .

The three terms on the right of Eq. (1) have clear physical significance. The first term reflects Beer's law that the change in  $L$  is proportional to  $L$ . The second (integral) term is a source term corresponding to the scattering of diffuse radiation from all directions into the particular

direction  $\mu\phi$ , and the last term is a source function corresponding to the scattering of radiation from the direct radiance component  $L_0$  into the direction  $\mu\phi$ .

Given the phase function  $p(\cos\psi)$ , its normalization constant  $\omega_0$  and the boundary conditions of Eqs. (6) and (7), the scattering problem described by Eq. (1) is fully defined. In principle, one solves this equation for  $L(\tau, \mu, \phi)$ . Then, an appropriate cloud reflection coefficient  $\rho(\text{sr}^{-1})$  is defined by

$$\rho(\mu, \phi) = \frac{L(0, \mu, \phi)}{E_0}, \quad \mu > 0. \quad (8)$$

In practice, the solution of Eq. (1) is formidable. The primary purpose of this paper is to investigate rational approximate solutions. Descriptions of the approximations comprise Section 4 of this report. For the most part, the difficulty in solving Eq. (1) is caused by the presence of the integral scattering source term, and the principle methods of approximation simplify this term. The first-order approximation of completely neglecting this term is the so-called single-scattering approximation and is also considered.

### 3. TEST CONDITIONS

The cloud standard is a plane-parallel, semi-infinite cumulus cloud composed of spherical water droplets. The size distribution of particle radii is described by<sup>(4, 5)</sup>

$$n(r) = ar^{\alpha} e^{-\beta r^{\gamma}} \quad (9)$$

where

$$a = N \left\{ \sqrt{\beta}^{(\alpha+1)/\gamma} / \Gamma \left( \frac{\alpha+1}{\gamma} \right) \right\}.$$

$$\beta = \frac{\alpha}{\gamma r_C^{\gamma}},$$

$N$  = particle density ( $\text{cm}^{-3}$ ),  $r_C$  = radius of peak distribution ( $\mu\text{m}$ ), and  $\alpha$  and  $\gamma$  are size parameters controlling the shape (e.g., width and skewness) of the distribution. For the present work,  $\alpha = 6$ ,  $\gamma = 1$  and  $r_C = 4\mu\text{m}$  are used and the resulting distribution  $f(r) = n(r)/N$  is shown in Fig. 2.

Necessary inputs to any nonempirical model of cloud reflectance are the scattering (total and differential) and absorption cross sections for single cloud particles. These parameters were computed according to standard Mie scattering theory<sup>(5, \*)</sup> and averaged over the size distribution of Eq. (1). The index of refraction for water was taken from Ref. (6) and is shown in Fig. 3. Results in the  $2-20\mu\text{m}$  spectral region for the total scattering ( $\sigma_s$ ), total absorption ( $\sigma_a$ ) and total extinction ( $\sigma_e = \sigma_s + \sigma_a$ ) cross sections are shown in Fig. 4. The differential scattering cross section  $d\sigma_s(\theta)/d\Omega$  as a function of scattering angle at  $\lambda = 2.70$  and  $4.35\mu\text{m}$  is shown in Fig. 5. A fundamental feature of the differential scattering cross sections (i.e., the phase function) evident in Fig. 5 is the strong probability for forward scattering. Advantage is taken of this feature in

\*S. J. Young, Calculation of Scattering Cross Sections for Clouds, ATM 75(5409-40)-5, The Aerospace Corporation, El Segundo, California, 9 June 1975.

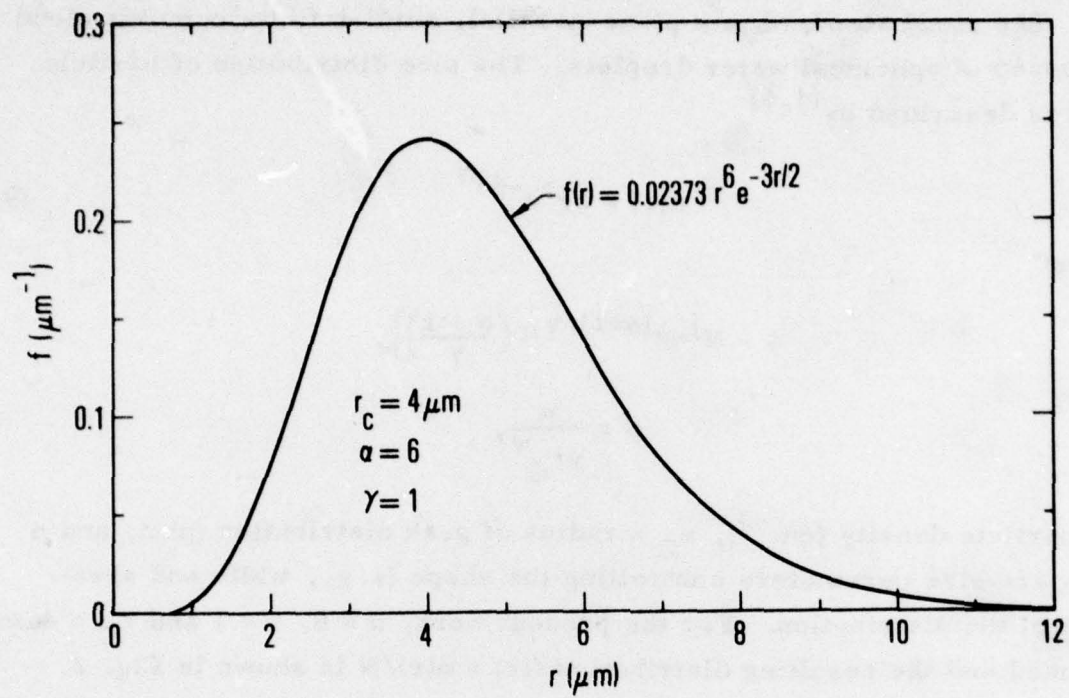
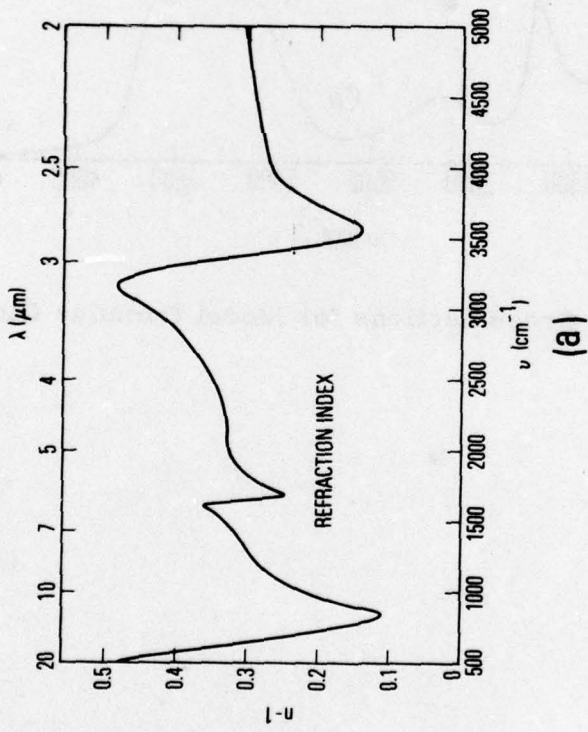
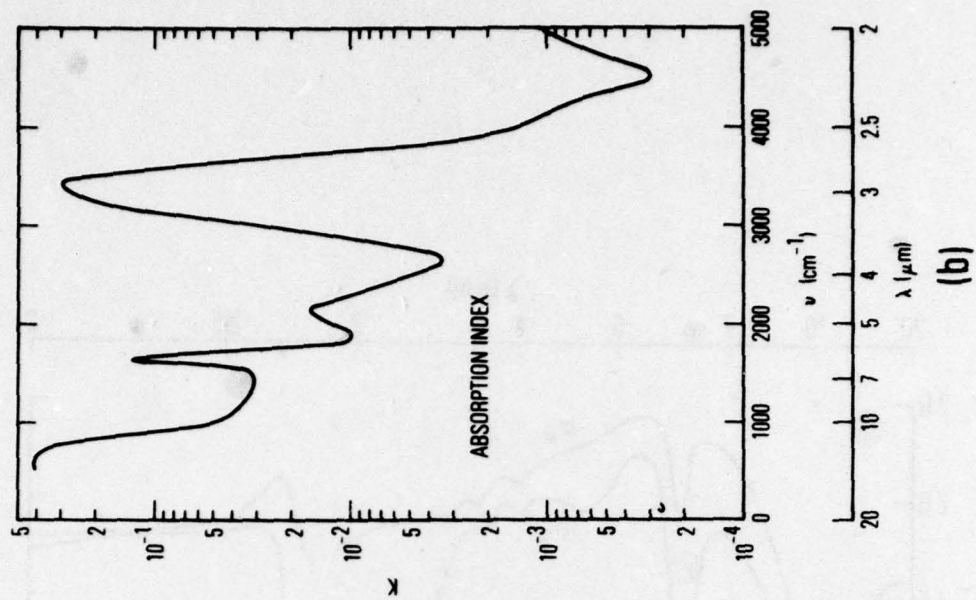


Fig. 2. Particle Size Distribution for Model Cumulus Cloud



(a)



(b)

Fig. 3. Index of Refraction of Water. (a) Real part. (b) Imaginary part.

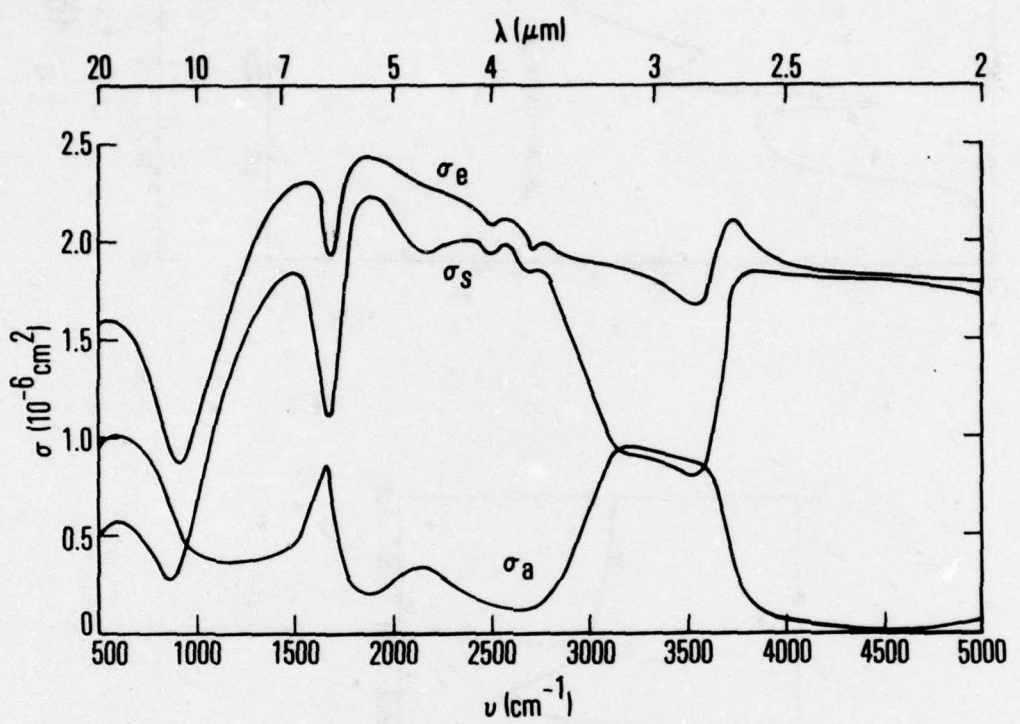


Fig. 4. Total Cross Sections for Model Cumulus Cloud

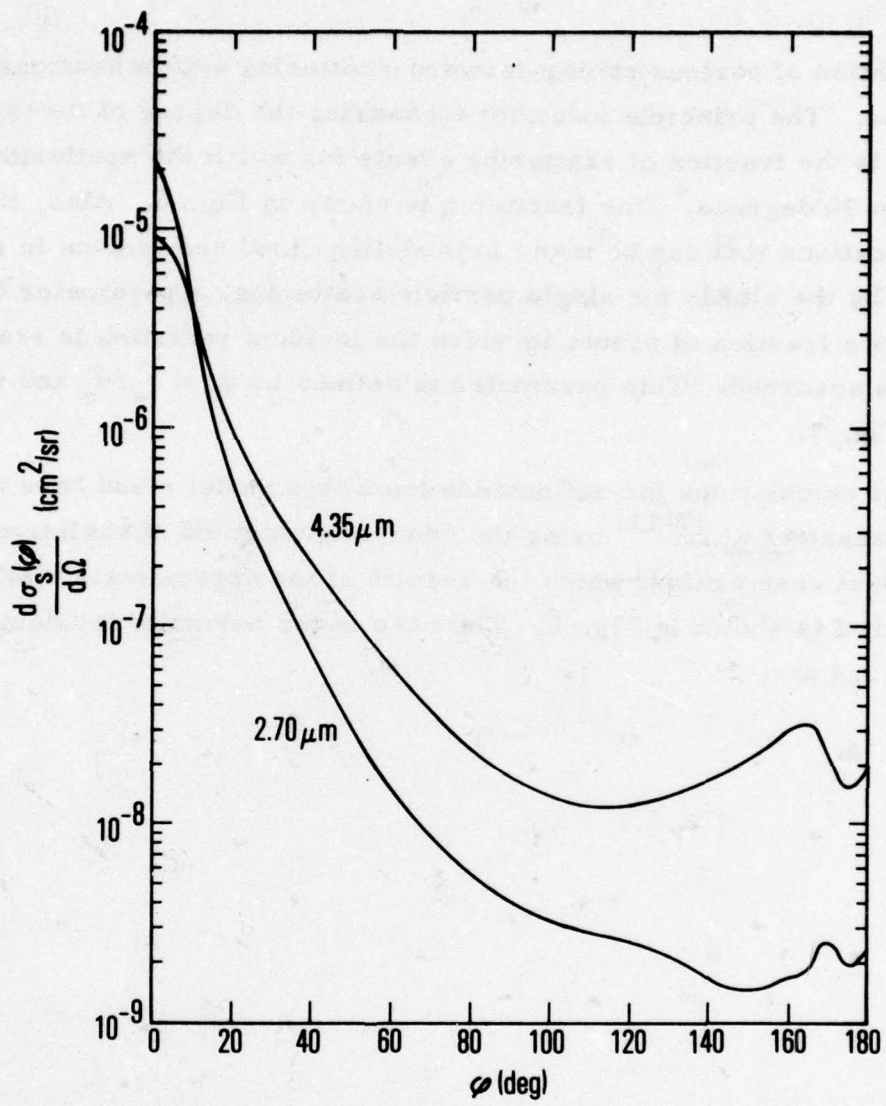


Fig. 5. Differential Scattering Cross Section for Model Cumulus Cloud

the formulation of various strong-forward-scattering approximations in the next section. The principle index for measuring the degree of forward scattering is the fraction of scattering events for which the scattering angle is less than 90 degrees. The fraction  $\eta$  is shown in Fig. 6. Also, the type of simplifications that can be made in modeling cloud reflectance is strongly influenced by the albedo for single particle scattering, a parameter that measures the fraction of events in which the incident radiation is scattered rather than absorbed. This parameter is defined by  $\omega_0 = \sigma_s / \sigma_e$  and is shown in Fig. 7.

Exact calculations for reflectance from this model cloud have been made by Hansen et al. (7-11) using the "doubling" method of radiative transfer. The test case against which the results of the approximate methods are compared is shown in Fig. 8. The case is for normally incident radiation at  $\lambda = 3.4 \mu\text{m}$ .

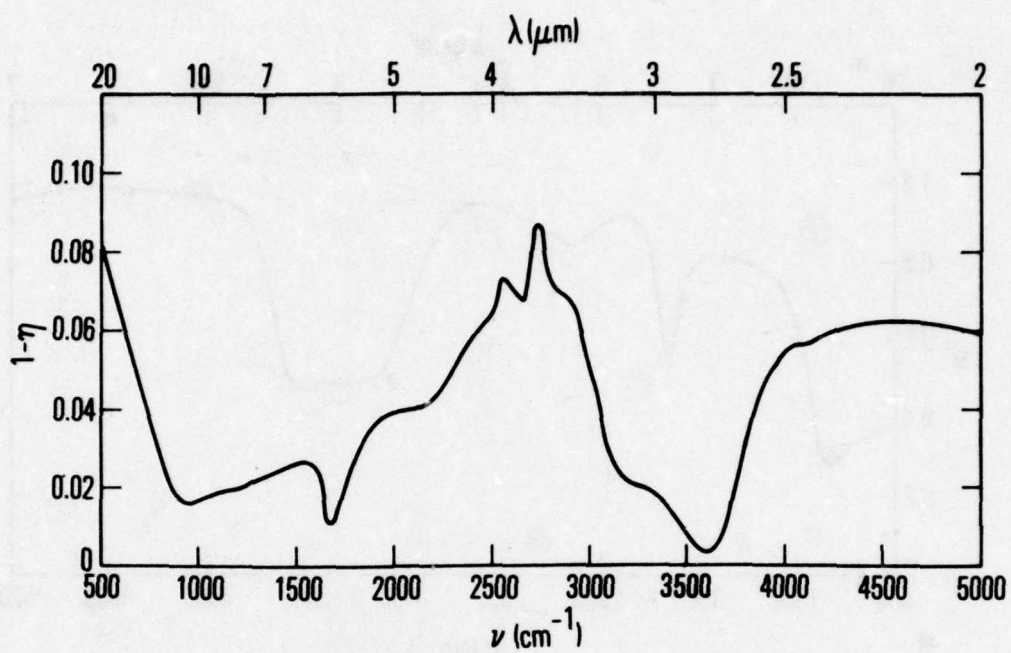


Fig. 6. Forward Scattering Parameter for Model Cumulus Cloud

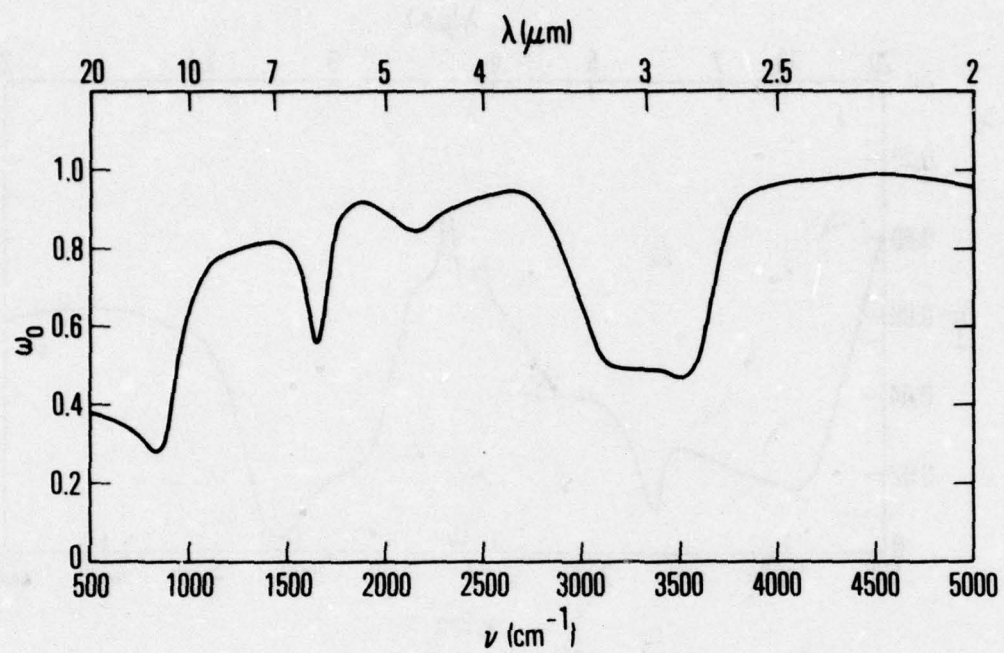


Fig. 7. Single Particle Scattering Albedo for Model Cumulus Cloud

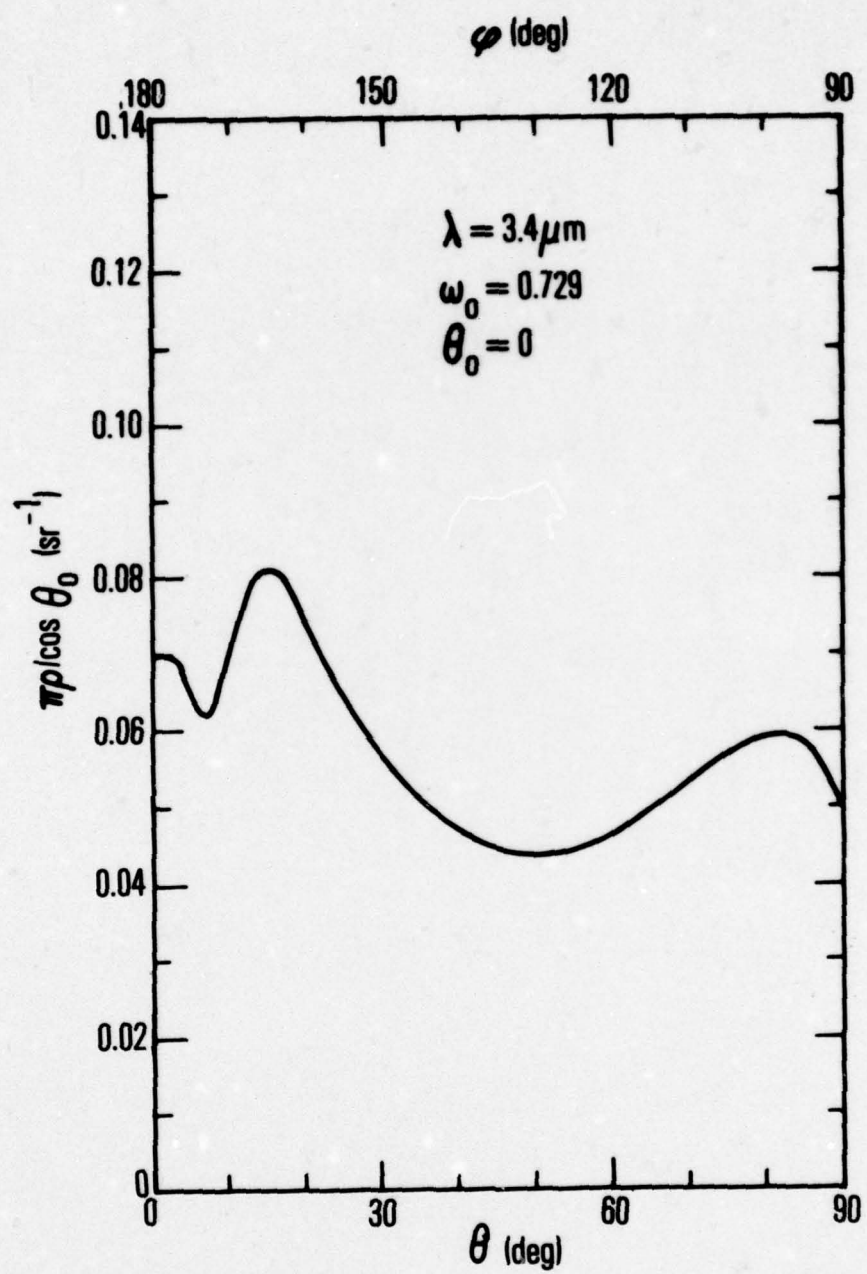


Fig. 8. Test Standard Cloud Reflectance

#### 4. MODEL DESCRIPTIONS AND RESULTS

##### A. Single-Scattering Model

The single-scattering model<sup>(12)</sup> for cloud reflectance considers the diffuse radiance field within the cloud to be composed only of those photons that have been scattered once from the primary incident beam. The radiative transfer equation for this condition is obtained from Eq. (1) by neglecting the integral source scattering term. The solution for  $L$  is obtained simply by solving the resulting first-order differential equation. The result for a semi-infinite cloud that satisfies the boundary conditions  $L(0, \mu, \phi) = 0$  for  $\mu < 0$  and  $L(\tau, \mu, \phi) \rightarrow 0$  for  $\tau \rightarrow \infty$  is

$$L(\tau, \mu, \phi) = \begin{cases} \frac{E_0}{4\pi} p(\cos\varphi_0) \left[ e^{-\tau/\mu_0} - e^{\tau/\mu} \right] \frac{\mu_0}{\mu + \mu_0} & \mu < 0 \\ \frac{E_0}{4\pi} p(\cos\varphi_0) e^{-\tau/\mu_0} \frac{\mu_0}{\mu + \mu_0} & \mu > 0 \end{cases} \quad (10)$$

where

$$\cos\varphi_0 = \cos(\phi - \phi_0) \sqrt{(1 - \mu^2)(1 - \mu_0^2) - \mu\mu_0}. \quad (11)$$

The reflection coefficient of Eq. (8) is then

$$\rho(\mu, \phi) = \frac{1}{4\pi} p(\cos\varphi_0) \frac{\mu_0}{\mu + \mu_0}. \quad (12)$$

The comparison of the prediction of this result with the standard test case is shown in Fig. 9. The single-scattering approximation under-predicts the reflectance by about a factor of three.

Although the single-scattering approximation fails as a general approximation, it has two redeeming features; (1) it is extremely simple to apply, and (2) it can be quite accurate in some spectral regions. The first feature is used to advantage in the formulation of modified single-scattering approximations (Sections B and C). Results from a previous

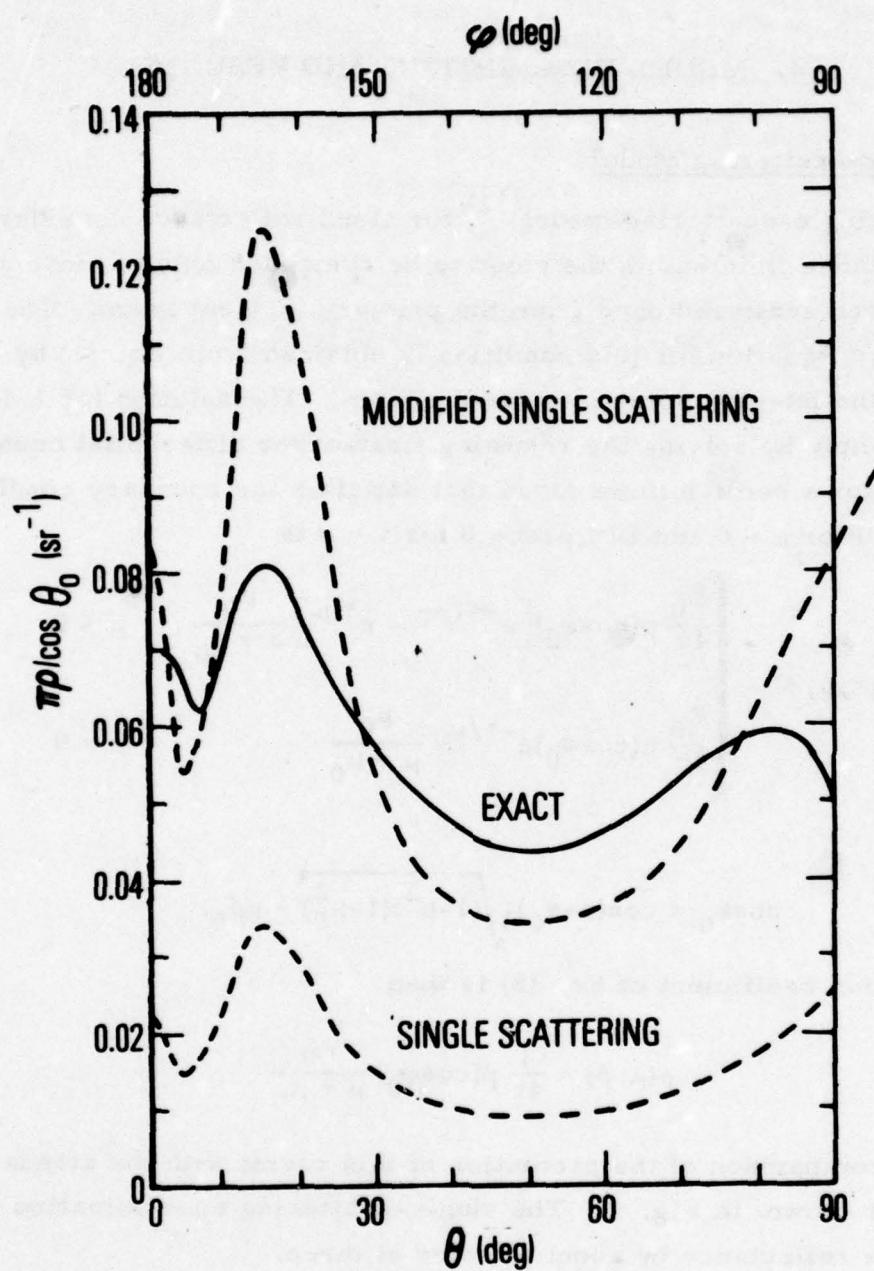


Fig. 9. Comparison of Single-Scattering Approximations with Test Case

study on cloud reflectance\* has established that this model is adequate for practical application in the 2- to 3- $\mu\text{m}$  spectral region. In Fig. 10, a comparison is made between the model and experimental field measurements.<sup>(13, 14)</sup> The measurements were made with an airborne sensor flying 1 km above a uniform cloud deck with an observation zenith angle of 80 degrees, a solar zenith angle of 88.5 degrees, and a nearly coplanar geometry for the entrance and exit rays (i.e.,  $\phi - \phi_0 = 0$ ). When proper account of atmospheric attenuation is made of the path from space, to the cloud, and back to the sensor, the agreement is quite good.

The success of the single-scattering model in the 2.7- $\mu\text{m}$  region can be attributed to the large value of the absorption coefficient of liquid water in this spectral region (Fig. 3b). This large value is carried over into a broad peak in the spectrum for the absorption cross section  $\sigma_a$  (Fig. 4) and, consequently, into a broad valley in the spectrum for the single-scattering albedo  $\omega_0$  (Fig. 7). The effect is that photons that must be scattered more than once in order to escape the top of the cloud in the desired reflection direction have a large probability of being absorbed rather than scattered. At  $\lambda = 3.4\text{-}\mu\text{m}$ , on the other hand, the absorptance by liquid water is small, and higher orders of scattering contribute significantly to the reflected radiation field.

#### B. Two-Stream Theoretical Modification of the Single-Scattering Model

The general development of radiative transfer in scattering media has produced a set of approximate solutions collectively known as "flux approximations." Among the more important are those due to Eddington, Schuster and Schwarzschild (two-stream approximation), and Sagan and Pollack (modified two-stream approximation). Use of these approximations for cloud reflectance has been considered by Irvine.<sup>(15)</sup> The essence of these approximations is the sacrifice of angular information of the

\* S. J. Young, Solar Scattering Calculations, ATM-75(5409-41)-3, The Aerospace Corporation, El Segundo, California, 14 December 1974.

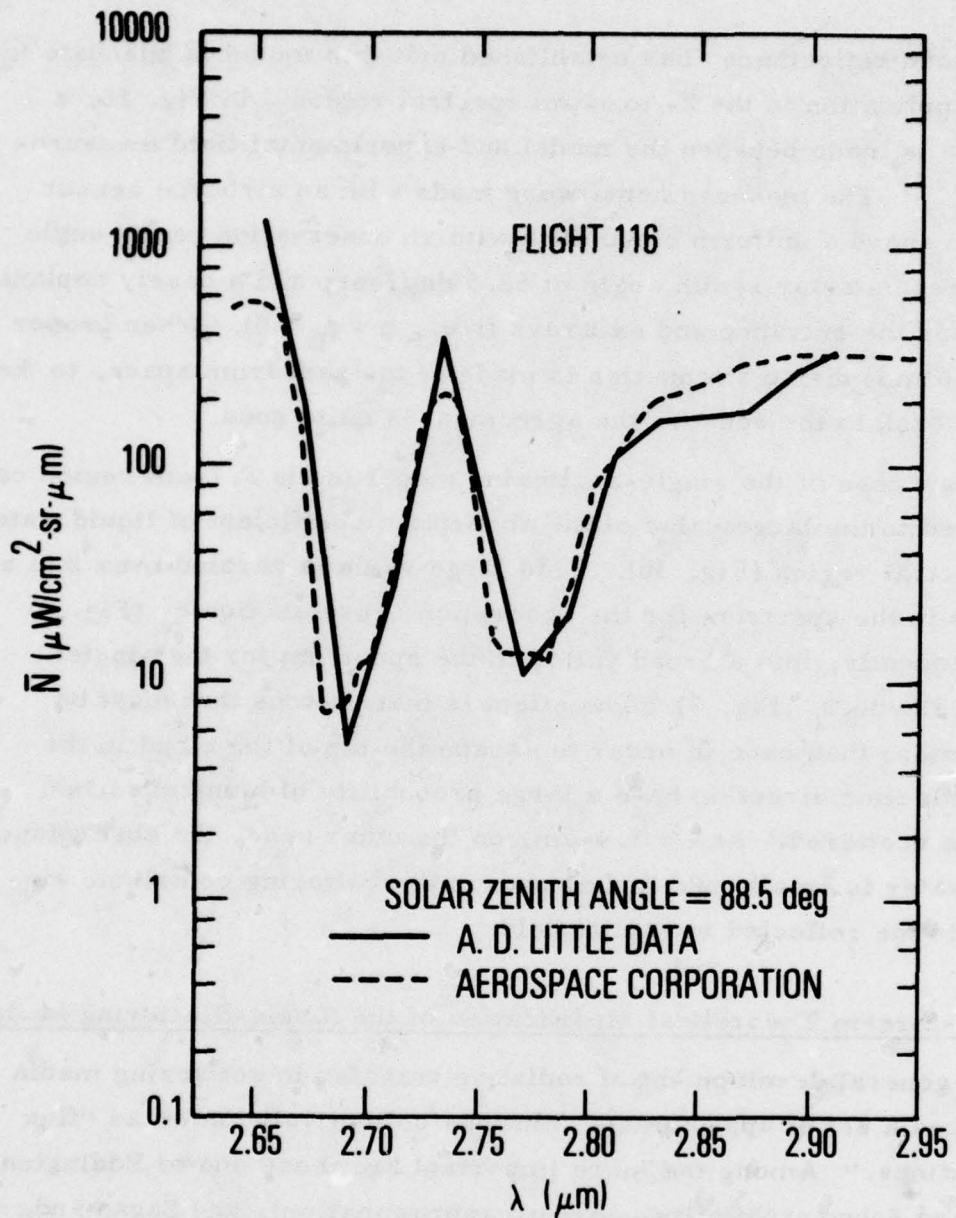


Fig. 10. Comparison between Single-Scattering Model and Experimental Data in the 2.7- $\mu\text{m}$  Spectral Region

general radiation field in order to efficiently compute the total flux in a given direction. In application to the cloud reflectance problem, these approximations yield only the albedo of the cloud, that is, only the total radiation reflected into the upper hemisphere. Because of this lack of angular information, these types of approximations are not considered here as final models. This approach is used, however, in order to derive an improvement on the simple single-scattering model.

The basic simplification made in Eq. (1) to obtain these flux approximations is to assume a phase function of the form

$$p(\mu, \phi, \mu', \phi') = 4\pi\omega_0 [\eta\delta(\mu' - \mu)\delta(\phi' - \phi) + (1 - \eta)\delta(\mu + \mu')\delta(\phi' - \pi - \phi)] \quad (13)$$

where  $\delta$  is the Dirac delta function. This form allows only direct forward and backscatter along the primed beam axis.  $\eta$  is the forward scattering parameter. The radiance field is similarly constructed as

$$L(\tau, \mu, \phi) = \frac{1}{\mu_0} [E^+(\tau)\delta(\mu - \mu_0)\delta(\phi - \pi - \phi_0) + E^-(\tau)\delta(\mu + \mu_0)\delta(\phi - \phi_0)]. \quad (14)$$

Thus, the field is assumed to contain components only in and opposed to the direction of the incident solar radiation.  $E^+$  and  $E^-$  are the radiance flux variables for the forward and backward directions, respectively. Substitution of Eq. (13) and (14) into Eq. (1) yields the following pair of coupled, first-order differential equations governing one-dimensional radiative transfer

$$\begin{aligned} \frac{dE^+(\tau)}{d\tau} &= \left[ \frac{1 - \eta\omega_0}{\mu_0} \right] E^+(\tau) - \left[ \frac{\omega_0(1 - \eta)}{\mu_0} \right] E^+(\tau) - \omega_0 E_0 (1 - \eta) e^{-\tau/\mu_0} \\ - \frac{dE^-(\tau)}{d\tau} &= \left[ \frac{1 - \eta\omega_0}{\mu_0} \right] E^-(\tau) - \left[ \frac{\omega_0(1 - \eta)}{\mu_0} \right] E^-(\tau) - \omega_0 E_0 \eta e^{-\tau/\mu_0}. \end{aligned} \quad (15)$$

The relevant boundary conditions are

$$E^-(0) = 0$$

and

$$E^\pm(\tau) \rightarrow 0 \text{ as } \tau \rightarrow \infty.$$

The solution of this set of equations yields<sup>(16)</sup>

$$\begin{aligned}\frac{E^+(\tau)}{E_0} &= \mu_0 r_0 e^{-k\tau/\mu_0} \\ \frac{E^-(\tau)}{E_0} &= \mu_0 [e^{-k\tau/\mu_0} - e^{-\tau/\mu_0}]\end{aligned}\quad (17)$$

where

$$k = \sqrt{(1-\omega_0)[1-(2\eta-1)\omega_0]}, \quad (18)$$

and

$$r_0 = \frac{k - (1-\omega_0)}{k + (1-\omega_0)}. \quad (19)$$

The reflection coefficient (total albedo) is obtained as

$$\rho = \frac{E^+(0)}{E_0} = \mu_0 r_0. \quad (20)$$

Adamson<sup>(16)</sup> has expanded  $r_0$  in orders of scattering to obtain

$$r_0 = \sum_{n=1}^{\infty} \rho_n \quad (21)$$

where

$$\rho_n = \omega_0^n \left(\frac{\eta}{2}\right)^n \frac{n}{1-\eta} \sum_{j=0}^{[n/2]} \frac{(2n-2j)!}{j!(n-j)!(n-2j+1)!} \left[-\frac{(2\eta-1)}{\eta^2}\right]^j. \quad (22)$$

The contributions to the albedo from once, twice, and three times scattered photons are, respectively

$$\rho_1 = \frac{\mu_0 \omega_0}{2^2} 2(1-\eta),$$

$$\rho_2 = \frac{\mu_0 \omega_0^2}{2^3} 2\eta 2(1-\eta), \quad (23)$$

and

$$\rho_3 = \frac{\mu_0 \omega_0^3}{2^4} \left[ (2\eta)^2 2(1-\eta) + \frac{2^3}{4} (1-\eta)^3 \right].$$

In the limit of strong forward scattering ( $\eta \rightarrow 1$ ), these contributions approach

$$\rho_1 \rightarrow \mu_0 \omega_0 \frac{(1-\eta)}{2},$$

$$\rho_2 \rightarrow \mu_0 \omega_0^2 \frac{(1-\eta)}{2}, \quad (24)$$

and

$$\rho_3 \rightarrow \mu_0 \omega_0^3 \frac{(1-\eta)}{2}$$

and, in general

$$\rho_n \rightarrow \mu_0 \omega_0^n \frac{(1-\eta)}{2}. \quad (25)$$

In this limit, one can calculate simply the ratio of all multiple scattering contributions to the first order (single-scattering) contribution as

$$C = \frac{\rho_1}{\sum_{n=2}^{\infty} \rho_n} = \frac{1}{1-\omega_0}. \quad (26)$$

Although this result has been obtained in the flux approximation, it is applied as a correction factor to the single-scattering result of Eq. (12) to obtain an improved model

$$\rho(\mu, \phi) = C \rho_{SS}(\mu, \phi) \quad (27)$$

where  $\rho_{SS}$  is the single-scattering approximation. The form of the correction factor is intuitively correct. As the probability for single scattering increases, i.e., as  $\omega_0$  increases towards unity, the effects of multiple scattering contributions to the reflectance must increase. This intuitive result is evident in the increase of the multiple-scattering correction factor  $C$  with  $\omega_0$ . This approximation must fail, however, for conservative scattering ( $\omega_0 \rightarrow 1$ ) since then  $\rho \rightarrow \infty$ . For the present application, this poses no problem since  $\omega_0$  never exceeds  $\sim 0.9$  (see Fig. 7).

For the test case condition of Fig. 8,  $\omega_0 = 0.729$  and the correction factor is  $C = 3.56$ . The product of  $C$  and  $\rho_{SS}$  is shown in Fig. 9. The agreement with the exact reflectance curve has been improved so that the maximum error, except at  $\theta = 90$  degrees, is only  $\sim 50$  percent.

### C. Empirical Modification of the Single-Scattering Model

Comparison of the predictions of the theoretically modified single-scattering model with exact calculations was extended beyond the single comparison of Fig. 9 in order to determine the range of its application. The exact results were obtained from Refs. 9 and 11. The results of this comparison are given in Table 1 and Fig. 11. Column one of Table 1 gives the wavelength of the eight cases used in the comparison. The second column lists the figure number and reference from which the exact result was obtained. The size distribution function of Eq. (9) with  $r_C = 4 \mu\text{m}$ ,  $\gamma = 1$  and  $\alpha = 6$  applies in all cases, but for three of the cases, the cloud particles were assumed to be spherical ice particles. The cloud particle type is listed in column three of the table. The fourth column tabulates the single-scattering albedo for the wavelength  $\lambda$ , the fifth column is the theoretical correction factor of Eq. (26), and the last column is the factor obtained from the exact results. This last factor was obtained from the figures referenced in the second column by computing the mean ratio between the exact and single-scattering reflectance over whatever variable

Table 1. Data for Construction of Empirically Modified  
Single-Scattering Model.

$\lambda(\mu\text{m})$	Fig. / Ref.	Cloud Type	$w_0$	$C=1/(1-w_0)$	Exact Factor
1.28	13/9	Water	0.9984	625	20
1.50			0.973	37	18
2.00			0.900	10	10
2.25	17/11		0.991	108	28
2.47	15/9	Ice	0.940	12	17
2.72			0.830	5.9	4.5
3.10			0.520	2.1	1.8
3.40	21/11	Water	0.729	3.7	3.4

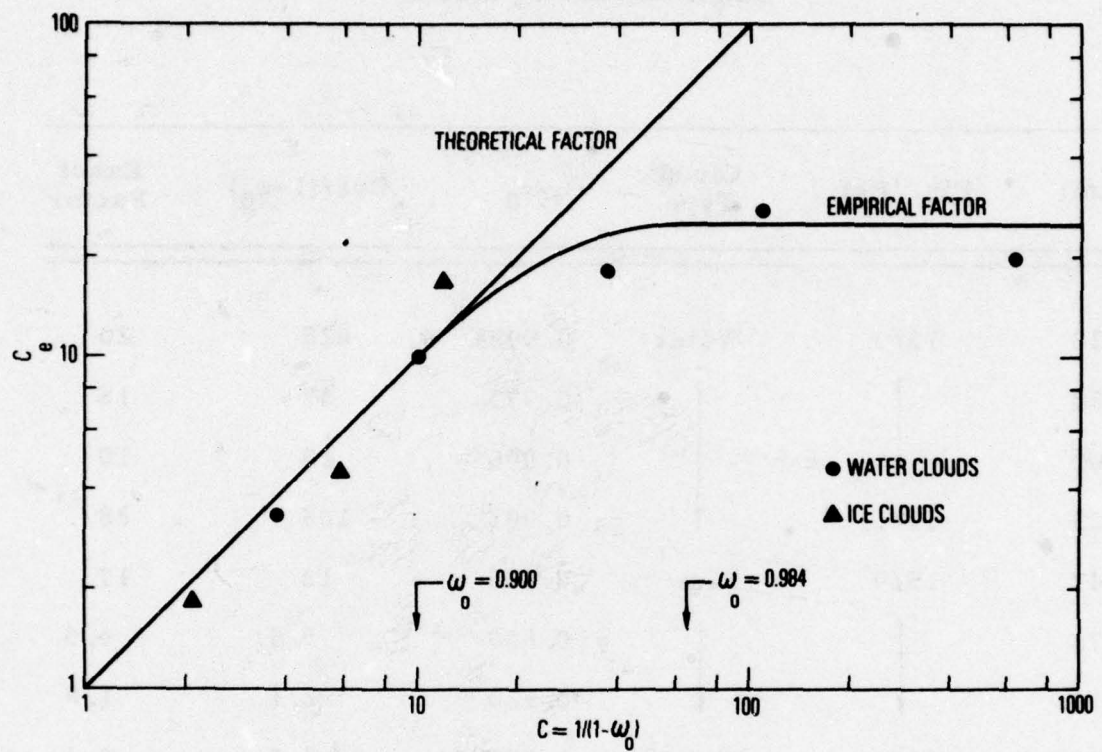


Fig. 11. Correction Factors for the Modified Single-Scattering Models

(e.g.,  $\theta$  or  $\phi$ ) was used to plot the results in Refs. 9 and 11. A plot of this exact factor versus the theoretical factor  $1/(1-\omega_0)$  is shown in Fig. 11. For  $\omega_0 \leq 0.9$  [ $1/(1-\omega_0) \leq 10$ ], the comparison between the model and exact results is very good. For more conservative scattering, however, the model overpredicts the multiple-scattering contribution to reflectance. The model predicts a continuing linear increase with  $1/(1-\omega_0)$  while the exact results indicate a saturation for  $\omega_0 \geq 0.99$  [ $1/(1-\omega_0) \geq 100$ ] such that the true reflectance is never more than 25 times larger than the single-scattering prediction. An empirically modified single-scattering model was thus constructed by taking the correction factor  $C_e$  to be its theoretical value for  $\omega_0 \leq 0.9$ , the saturation value  $C_e = 25$  for  $\omega_0 \geq 0.984$ , and the interpolated value

$$C_e = 10^F \quad (28)$$

with

$$F = 1.3979 - 0.6282 \left[ \log_{10} \left( \frac{0.0160}{1-\omega_0} \right) \right]^2 \quad (28)$$

for  $0.900 \leq \omega_0 \leq 0.984$ . This correlation for  $C_e$  is the curve labeled Empirical Factor in Fig. 11. In all, the approximation appears to be accurate to  $\pm 50$  percent for most cases, with an occasional excursion to a factor of two error.

An example of the application in the 2- to 20- $\mu\text{m}$  region of the single-scattering, theoretically modified single-scattering and empirically modified single-scattering models is shown in Fig. 12. The sun is at the zenith and the observation is at the coplanar 45 degrees zenith.

#### D. Turner Model

Turner<sup>(3,17,18)</sup> has developed and applied a multiple-scattering model that is developed along the lines of the flux approximations, but which retains the dependence of the reflectance on the entrance and exit zenith angles. In effect, this model is the next logical step after the flux

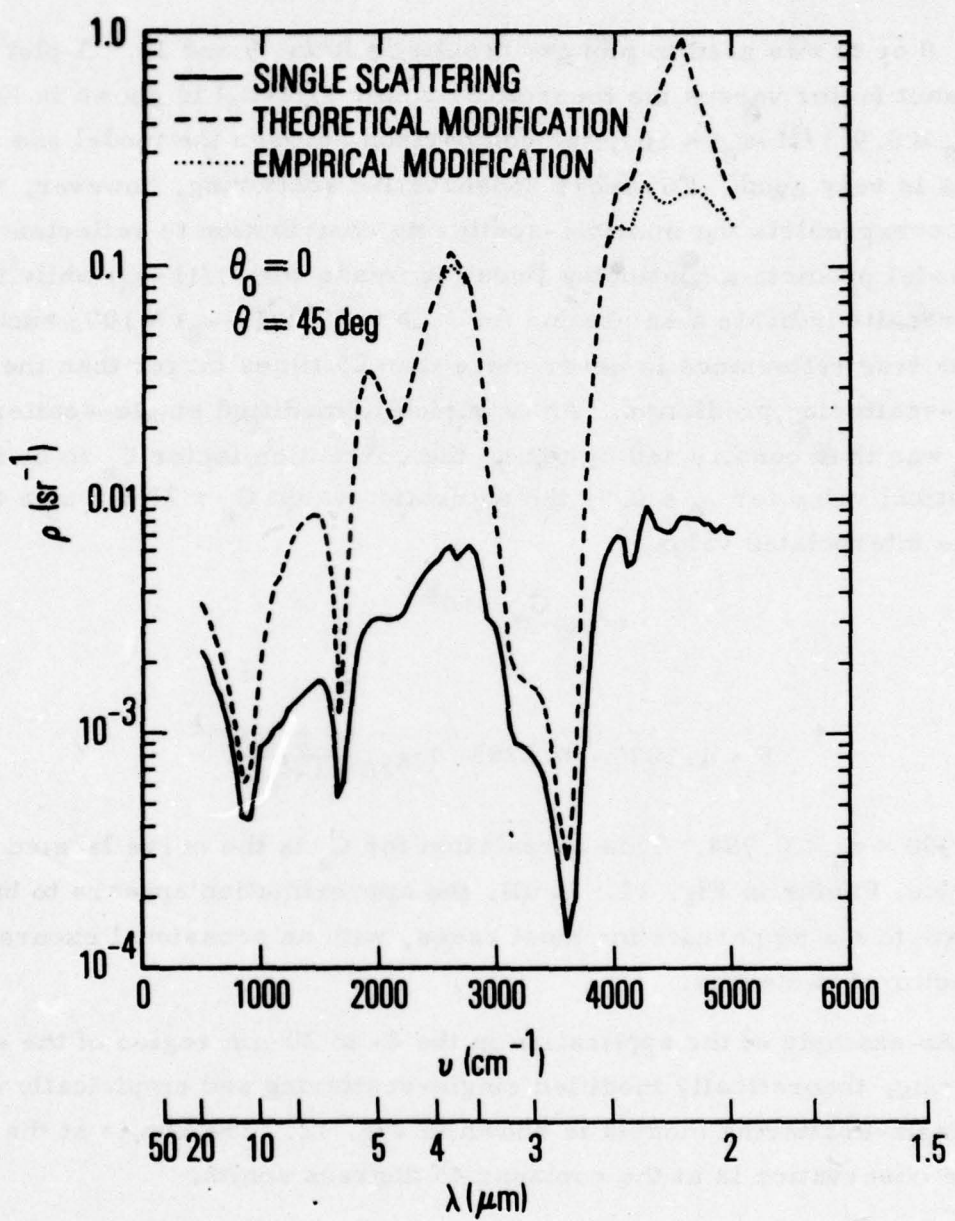


Fig. 12. Predicted Cloud Reflectance with Single-Scattering and Modified Single-Scattering Models

approximations. The solutions for  $E^\pm(\tau)$  of Eq. (17) are substituted into Eq. (14) for  $L(\tau, \mu, \phi)$  and this result, in turn, substituted into the radiative transfer equation [Eq. (1)]. Equation (13) for  $p(\mu, \phi, \mu', \phi')$  is also substituted into Eq. (1), but this time, only into the integral scattering term. Integration over the angular variables in the integral scattering term reduces Eq. (1) to a linear first-order differential equation for which the solution is (for a semi-infinite cloud)

$$L(\tau, \mu, \phi) = \begin{cases} \frac{E_0}{4\pi} [p(\cos\varphi_0) + r_0 p(-\cos\varphi_0)] \frac{\mu_0}{\mu_0 + k\mu} \{e^{-k\tau/\mu_0} - e^{\tau/\mu}\} & \mu < 0 \\ \frac{E_0}{4\pi} [p(\cos\varphi_0) + r_0 p(-\cos\varphi_0)] \frac{\mu_0}{\mu_0 + k\mu} e^{-k\tau/\mu_0} & \mu > 0 \end{cases} \quad (29)$$

from which the reflection coefficient is obtained as

$$p(\mu, \phi) = \frac{1}{4\pi} [p(\cos\varphi_0) + r_0 p(-\cos\varphi_0)] \frac{\mu_0}{\mu_0 + k\mu} \quad \mu > 0 \quad (30)$$

where  $\varphi_0$  is defined by Eq. (11),  $k$  by Eq. (18), and  $r_0$  by Eq. (19).

The significant feature of this model is that it augments the contribution from single-scattering by adding a "backscatter component," that is, the component  $r_0 p(-\cos\varphi_0)$ . The prediction of this model for the standard test case is shown in Fig. 13. For this normal incident case, the principle failing of the model is evident—a gross overprediction of the reflectance results for direct back reflection ( $\theta = 0$ ). This results because the Turner model's "backscatter" contribution to the single-scattering contribution is, in fact, the strong forward scattering lobe of the phase function. For large exit zenith angles, this model adds little to the predictions of the single-scattering model (compare Figs. 9 and 13 for  $\theta \approx 90$  degrees).

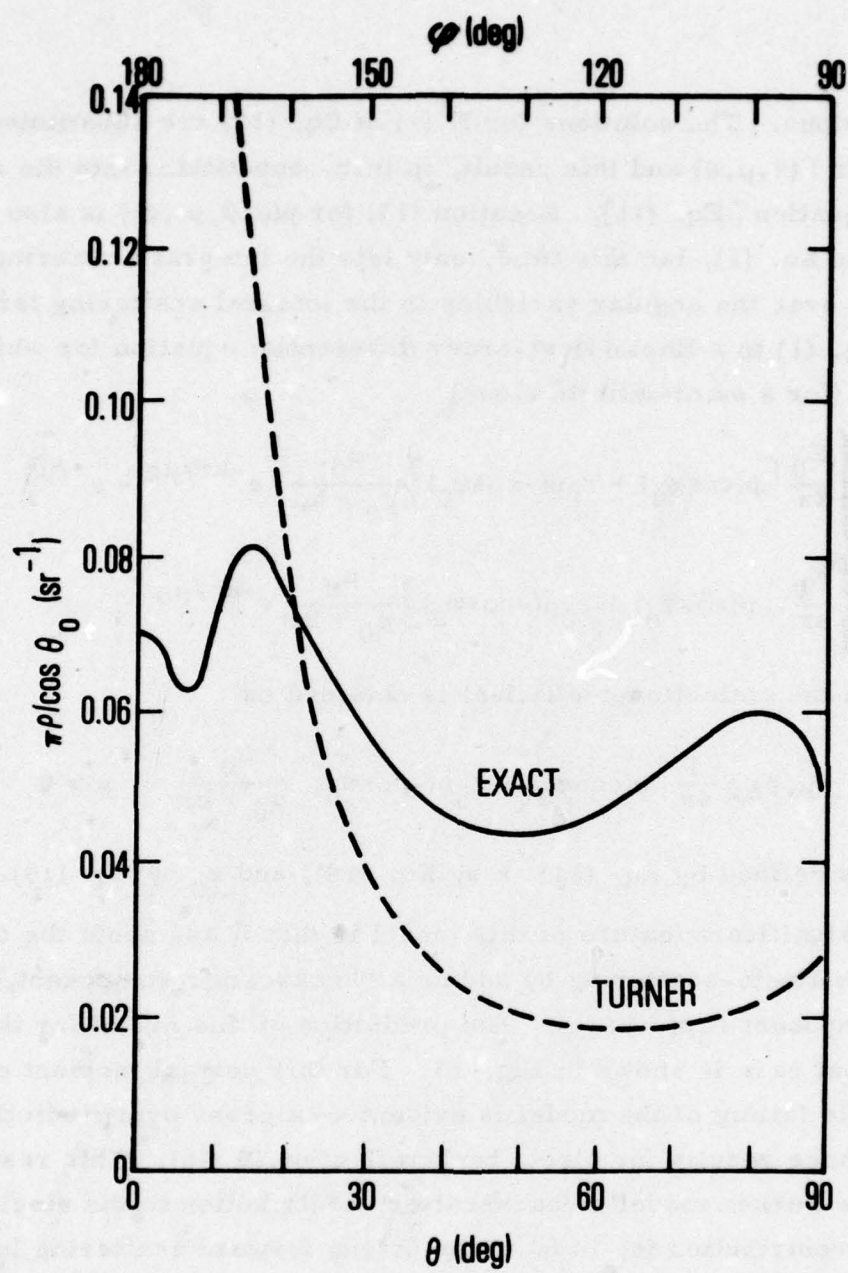


Fig. 13. Comparison of Turner Model Prediction with Test Case

### E. Romanova Approximation

For scattering problems involving phase functions that are strongly peaked in the forward direction, Romanova<sup>(19-21)</sup> gives a procedure for separating the general transfer equation into two parts. One part describes the strongly angle-dependent forward radiation field, while the other describes the weakly angle-dependent remainder field. The separation is effected by rewriting the transfer equation [Eq. (1)] as

$$-\mu_0 \frac{dL(\tau, \mu, \phi)}{d\tau} = L(\tau, \mu, \phi) - \frac{1}{4\pi} \int_0^{2\pi} \int_{-1}^1 p(\mu, \phi, \mu', \phi') L(\tau, \mu', \phi') d\mu' d\phi' \\ - \frac{E_0}{4\pi} e^{-\tau/\mu_0} p(\mu, \phi, -\mu_0, \phi_0) - \epsilon(\mu_0 + \mu) \frac{dL(\tau, \mu, \phi)}{d\tau}. \quad (31)$$

When the parameter  $\epsilon$  is set to unity, the exact transfer equation is recovered. When  $\epsilon = 0$ , the equation describes the field in the direction  $\mu = -\mu_0$ . The field variable  $L(\tau, \mu, \phi)$  is now decomposed by

$$L(\tau, \mu, \phi) = L_1(\tau, \mu, \phi) + \epsilon L_2(\tau, \mu, \phi) \quad (32)$$

and substituted into Eq. (31). Collecting terms independent of  $\epsilon$  yields the following transfer equation for  $L_1$

$$-\mu_0 \frac{dL_1(\tau, \mu, \phi)}{d\tau} = L_1(\tau, \mu, \phi) - \frac{1}{4\pi} \int_0^{2\pi} \int_{-1}^1 p(\mu, \phi, \mu', \phi') L(\tau, \mu', \phi') d\mu' d\phi' \\ - \frac{E_0}{4\pi} e^{-\tau/\mu_0} p(\mu, \phi, -\mu_0, \phi_0). \quad (33)$$

Collecting terms containing  $\epsilon$  and setting  $\epsilon = 1$  yields the following transfer equation for  $L_2$

$$\mu \frac{dL_2(\tau, \mu, \phi)}{d\tau} = L_2(\tau, \mu, \phi) - \frac{1}{4\pi} \int_0^{2\pi} \int_{-1}^1 p(\mu, \phi, \mu', \phi') L_2(\tau, \mu', \phi') d\mu' d\phi' \\ - (\mu_0 + \mu) \frac{dL_1(\tau, \mu, \phi)}{d\tau} \quad (34)$$

Presumably, Eq. (33) describes the field in the direction  $\mu = -\mu_0$  and  $\phi = \phi_0$  (which is strongly angle dependent, at least for  $\tau$  not too large) and Eq. (34) describes a field that is relatively slowly varying with angle. The original transfer equation is recovered by adding Eqs. (33) and (34).

Along with this separation, the boundary conditions are also modified. In particular, a condition is placed on  $L_1$  that suppresses back-scattering. That is,  $L_1(0, \mu, \phi) = 0$  for  $\mu > 0$ . Coupled with the condition  $L_1(0, \mu, \phi) = 0$  for  $\mu < 0$  imposed by the fact that  $L_1$  is a diffuse field yields the general result  $L_1(0, \mu, \phi) = 0$  for all  $\mu$ . This diffusivity agreement also requires  $L_2(0, \mu, \phi) = 0$  for  $\mu < 0$ . In addition, both  $L_1$  and  $L_2$  must remain finite for  $\tau \rightarrow \infty$ .

The method of solution for  $L_1$  is complicated, and is only sketched out here. Standard<sup>(2)</sup> expansions of both  $L_1$  and  $p$  are made. The azimuth angle variation is handled by expansion in a series of cosine functions of the form  $\cos m\phi$  and the zenith angle variation by expansion in a series of associated Legendre polynomials  $P_\ell^m(\mu)$ . When these expansions are substituted into the radiative transfer equation [Eq. (1)], a first order differential equation for the optical depth dependent expansion coefficients  $L_1^{\ell m}(\tau)$  can be isolated. This equation is solved subject to the boundary condition  $L_1^{\ell m}(0) = 0$  for all  $\mu$ . The solution is then substituted back into the expansions over  $\ell$  and  $m$ . The resulting form can then be summed explicitly over  $m$  to obtain the final solution

$$L_1(\tau, \mu, \phi) = \frac{E_0}{4\pi} e^{-\tau/\mu_0} \sum_{\ell=0}^N (2\ell+1) P_\ell(\cos\phi_0) \left[ \exp\left\{\frac{\omega_\ell}{2\ell+1} \frac{\tau}{\mu_0}\right\} - 1 \right] \quad (35)$$

where  $\omega_\ell$  are the expansion coefficients

$$\omega_\ell = \frac{2\ell+1}{2} \int_{-1}^1 p(x) P_\ell(x) dx \quad (36)$$

for the expansion of  $p$  in Legendre polynomials

$$p(\cos\phi) = \sum_{\ell=0}^N \omega_\ell P_\ell(\cos\phi). \quad (37)$$

This contribution to the total field  $L$  cannot contribute directly to the reflectance since  $L_1(0, \mu, \phi) = 0$  for all  $\mu$ . This solution is required, however, in the solution for  $L_2$ . The significant advantage of this approximation is that since  $L_2$  is assumed to be a slowly varying field with angle, the solution of Eq. (34) is substantially easier to obtain by standard techniques<sup>(22)</sup> than Eq. (1) is for the original field  $L$ . The simplest case, that is, when  $L_2$  is nearly isotropic, is considered here. If  $L_2$  is assumed independent of the angle variables in the integral source term of Eq. (34), then the resulting transfer equation for  $L_2$  is

$$\mu \frac{dL_2(\tau, \mu, \phi)}{d\tau} = (1 - \omega_0)L_2(\tau, \mu, \phi) - (\mu_0 + \mu) \frac{dL_1(\tau, \mu, \phi)}{d\tau}. \quad (38)$$

The solution of this first-order differential equation that satisfies the boundary condition  $L_2(0, \mu, \phi) = 0$  for  $\mu < 0$  is

$$L_2(\tau, \mu, \phi) = -\frac{(\mu + \mu_0)}{\mu} L_1(\tau, \mu, \phi) + \frac{(\mu + \mu_0)(1 - \omega_0)}{\mu^2} \frac{E_0}{4\pi} \times \\ \times \sum_{\ell=0}^N (2\ell + 1) P_\ell(\cos\phi_0) \left[ \frac{\exp\left\{-\left(1 - \frac{\omega_\ell}{2\ell + 1}\right) \frac{\tau}{\mu_0}\right\}}{\left[\frac{1 - \omega_0}{\mu} + \left(1 - \frac{\omega_\ell}{2\ell + 1}\right) \frac{1}{\mu_0}\right]} - \frac{\exp\left\{-\left(1 - \omega_0\right) \frac{\tau}{\mu} - \frac{\tau}{\mu_0}\right\}}{\left[\frac{1 - \omega_0}{\mu} + \frac{1}{\mu_0}\right]}\right]. \quad (39)$$

Finally then, the reflection coefficient is [Eq. (8)]

$$\rho(\mu, \phi) = \frac{\mu_0(\mu + \mu_0)(1 - \omega_0)}{4\pi[(1 - \omega_0)\mu_0 + \mu]} \sum_{\ell=0}^N \frac{\omega_\ell P_\ell(\cos\phi_0)}{\left[(1 - \omega_0)\mu_0 + \left\{1 - \frac{\omega_\ell}{2\ell + 1}\right\}\mu\right]}. \quad (40)$$

Application of this result for  $\rho(\mu, \phi)$  requires the decomposition of the phase function into a series of Legendre polynomials according to Eqs. (36) and (37). This decomposition is considered to be too complicated

for a model such as we are trying to formulate here. Since we have assumed all along that  $p(\varphi)$  is a strongly forward-peaked function, we will continue with this assumption for the final simplification of  $\rho(\mu, \phi)$ . Consider the analytic Henyey-Greenstein phase function<sup>(15)</sup>

$$p(\varphi) = \frac{(1-\eta^2)w_0}{[1 - 2\eta \cos \varphi + \eta^2]^{3/2}} \quad (41)$$

whose expansion coefficients are

$$w_\ell = w_0 \eta^\ell (2\ell+1). \quad (42)$$

In the limit  $\eta \rightarrow 1$ , this function represents a strongly forward-peaked function and  $w_\ell \rightarrow w_0 (2\ell+1)$ . If this result is used in the denominator of Eq. (38) and Eq. (39) used to evaluate the sum, then  $\rho(\mu, \phi)$  is simplified to the final result

$$\rho(\mu, \phi) = \frac{p(\cos \varphi_0)}{4\pi} \frac{\mu + \mu_0}{\mu + (1-w_0)\mu_0}. \quad (43)$$

The prediction of this model for the standard test case conditions is shown in Fig. 14. Some improvement over the simple single-scattering model is evident, but on the whole the model does not meet the general criterion of a factor of two accuracy. Further discussion on this model is given in Section G.

#### F. Truncation Approximation

Hansen<sup>(8)</sup> and Potter<sup>(23)</sup> consider a straightforward approximation based on a simple, but physically justifiable, redefinition of the problem. Consider a phase function  $p(x)$  that is strongly peaked in the forward direction (note,  $x = \cos \varphi$ ,  $\varphi = \text{scattering angle}$ ) and normalized by Eq. (3) to

$$\int_{-1}^1 p(x) dx = 2w_0. \quad (44)$$

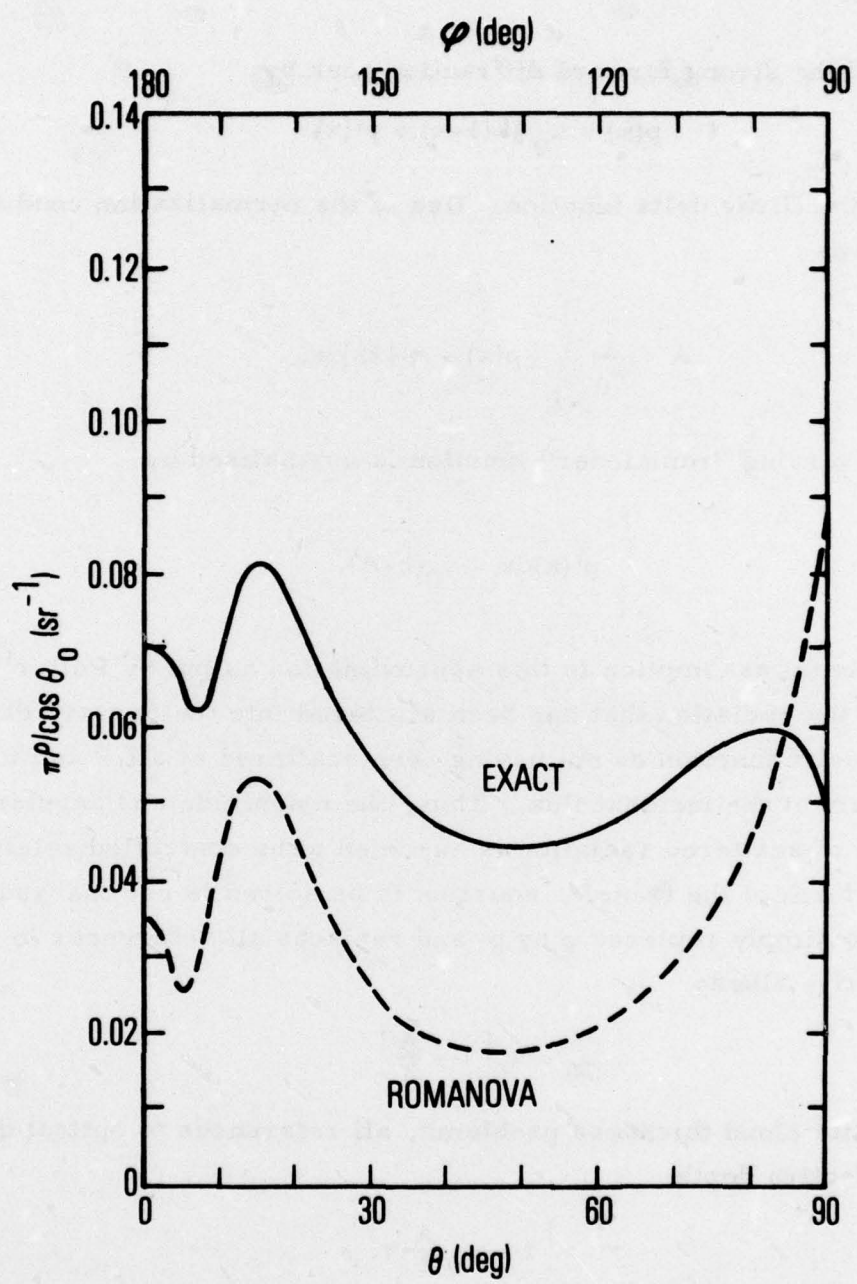


Fig. 14. Comparison of Romanova-isotropic Model Predicted with Test Case

Separate off the strong forward diffraction peak by

$$p(x) = \omega_0 A \delta(1-x) + p'(x) \quad (45)$$

where  $\delta$  is the Dirac delta function. Use of the normalization condition Eq. (44) gives

$$A = \frac{1}{\omega_0} \int_{-1}^1 [p(x) - p'(x)] dx. \quad (46)$$

The slowly varying "remainder" function is normalized by

$$\int_{-1}^1 p'(x) dx = \omega_0 (2-A). \quad (47)$$

The fundamental assumption in this approximation as put by Potter<sup>(23)</sup> is to "treat the radiation that has been scattered into the forward direction by the delta function as not having been scattered at all," and to still be a part of the incident flux. Thus, the magnitude and angular distribution of scattered radiation is assumed to be controlled solely by  $p'(x)$ . The form of the transfer equation to be solved is not changed. In Eq. (1), one simply replaces  $p$  by  $p'$  and replaces all references to  $\omega_0$  by the effective albedo

$$\omega'_0 = \omega_0 \left[ 1 - \frac{A}{2} \right] \quad (48)$$

and, for finite cloud thickness problems, all references to optical depth  $\tau$  by the effective depth

$$\tau' = \left[ 1 - \omega_0 \frac{A}{2} \right] \tau. \quad (49)$$

Since  $p'(x)$  is much less rapidly varying with angle than is  $p(x)$ , the solution of the transformed problem is much simpler.

The drawback of the method is that the truncation of the forward diffraction peak is a subjective choice. Most applications of the method have been made in the visible portion of the spectrum where the forward peak is extremely sharp and little judgment is required to determine the best truncation. In the infrared, though still strongly peak, the truncation of  $p(x)$  is ambiguous. Because of this ambiguity, the method is not pursued further.

#### G. Expansion in Orders of Scattering

The essence of this approximation is an approximate expansion of the radiation field in orders of scattering. This method has been described recently by Chou<sup>(24)</sup> and, for the most part, the development here follows that reference. Associated with each order (i.e., once, twice, three times, etc. scattered photons) is an azimuth independent source function  $Q_k(\tau, \mu)$  and an effective phase function  $p_k(\mu, \phi, -\mu_0, \phi_0)$  that is independent of  $\tau$ . The field is expanded as

$$L(\tau, \mu, \phi) = \sum_{k=1}^{\infty} Q_k(\tau, \mu) p_k(\mu, \phi, -\mu_0, \phi_0). \quad (50)$$

The first-order source function and effective phase function are obtained from the single-scattering solution of Eq. (10) as

$$Q_1(\tau, \mu) = \begin{cases} \frac{E_0}{4\pi} \left[ e^{-\tau/\mu_0} - e^{\tau/\mu} \right] \frac{\mu_0}{\mu + \mu_0} & \mu < 0 \\ \frac{E_0}{4\pi} e^{-\tau/\mu_0} \frac{\mu_0}{\mu + \mu_0} & \mu > 0 \end{cases} \quad (51)$$

and

$$p_1(\cos\phi_0) = p(\cos\phi_0). \quad (52)$$

The expansion of  $L(\tau, \mu, \phi)$  by Eq. (50) is substituted into the transfer equation Eq. (1) and the following approximations made. First,  $Q_k(\tau, \mu')$  in the integral source term is assumed to be independent of  $\mu'$ , taken outside the integral sign and evacuated at  $\mu' = \mu$ . \* Second, the effective phase functions are defined by the recurrence relation

$$p_k(\mu, \phi, -\mu_0, \phi_0) = \int_0^{2\pi} \int_{-1}^1 p(\mu, \phi, \mu', \phi') p_{k-1}(\mu', \phi', -\mu_0, \phi_0) d\mu' d\phi'. \quad (53)$$

This procedure, along the definition

$$Q_0(\tau, \mu) = E_0 e^{-\tau/\mu_0} \quad (54)$$

leads to the following differential equation for the source functions for  $k \geq 0$

$$\mu \frac{dQ_{k+1}(\tau, \mu)}{d\tau} - Q_k(\tau, \mu) = -\frac{1}{4\pi} Q_k(\tau, \mu). \quad (55)$$

By working out the solution for the first few values of  $k$ , one is led by induction to the following solution that satisfies the boundary conditions

$Q_k(0, \mu) = 0$  for  $\mu < 0$  and  $Q_k(\tau, \mu) \rightarrow 0$  as  $\tau \rightarrow \infty$

$$Q_k(\tau, \mu) = E_0 \left[ \frac{1}{4\pi} \frac{\mu_0}{\mu + \mu_0} \tau^k e^{-\tau/\mu_0} + e^{\tau/\mu} \sum_{j=0}^{k-1} \frac{(-1)^j C_{k-j} \left( \frac{\tau}{4\pi\mu} \right)^j}{j!} \right] \quad (56)$$

where

$$C_n = \begin{cases} -E_0 \left( \frac{1}{4\pi} \frac{\mu_0}{\mu + \mu_0} \right)^n & \mu < 0 \\ 0 & \mu > 0. \end{cases} \quad (57)$$

---

\*This assumption is the major simplification of Chou's method. He assumes this to be true over the upward and downward hemispheres only. Here, the assumption of isotropy is made.

This result gives the source functions for use in Eq. (50).

An expression for  $p_k(\cos\varphi_0)$  to be used in Eq. (50) is obtained by substituting the Legendre polynomial expansion of Eq. (37) for  $p(\cos\varphi_0)$  into Eq. (53). The result is

$$p_k(\cos\varphi_0) = \frac{1}{4\pi} \sum_{\ell=0}^N (2\ell+1) \left[ 4\pi \frac{\omega_\ell}{2\ell+1} \right]^k P_\ell(\cos\varphi_0). \quad (58)$$

The reflection coefficient is now obtained by substituting Eqs. (56) and (58) into (50), evaluating at  $\tau = 0$  for  $\mu > 0$  and dividing by  $E_0$ . The result is

$$\rho(\mu, \phi) = \frac{1}{4\pi} \sum_{\ell=0}^N C_\ell (2\ell+1) P_\ell(\cos\varphi_0)$$

where

$$C_\ell = \frac{\left( \frac{\omega_\ell}{2\ell+1} \right) \left( \frac{\mu_0}{\mu+\mu_0} \right)}{1 - \left( \frac{\omega_\ell}{2\ell+1} \right) \left( \frac{\mu_0}{\mu+\mu_0} \right)}. \quad (59)$$

Like the Romanova approximation, application of this model would require the expansion of  $p(\cos\varphi_0)$  in a series of Legendre functions. We simplify the model as in the Romanova approximation by use of Eq. (50) for  $\omega_\ell$  in the limit of strong forward scattering ( $\eta \rightarrow 1$ ). The result is, in fact, the same as that obtained in Eq. (51) for the Romanova approximation, and the consideration of accuracy is hence the same as made in Section E.

## 5. SUMMARY

The principle objective of this work has been to formulate and assess simple models for computing the diffuse reflectance of solar radiation from plane-parallel cloud layers. By "simple," is meant the ability to compute the reflectance from no more than the Mie scattering parameters and some algebraic formula. The most successful model is the empirically modified single-scattering model. The nominal error of the model is  $\pm 50$  percent. Several other models were considered (without empirical correction) but could either not achieve suitable accuracy in their simplest form (e.g., Romanova and orders of scattering), were too simple in their conception (e.g., Turner), or were ambiguous in application (e.g., truncation method). These results are summarized in Table 2.

Table 2. Summary of Reflectance Models.

Model	Comments
Single-Scattering	Fails for $\omega_0 \geq 0.5$
Single-Scattering with Theoretical Modification	Fails for $\omega_0 \geq 0.9$
Empirically Corrected Single-Scattering	Good for all $\omega_0$
Turner (two-stream approximation)	Fails for backscatter
Order of Scattering-Isotropic	Underestimates effects of multiple scattering
Romanova-Isotropic	Underestimates effects of multiple scattering
Diffraction Peak Truncation	Manner of truncation is ambiguous

## REFERENCES

1. R. M. Goody, Atmospheric Radiation. I. Theoretical Basis, The Clarendon Press, Oxford, 1964, p. 44.
2. S. Chandrasekhar, Radiative Transport, Dover Publications, New York, 1960.
3. A. J. LaRocca and R. E. Turner, Atmospheric Transmittance and Radiance: Methods of Calculation, Rpt. No. 107600-10-T, Environmental Research Institute of Michigan, Ann Arbor, Michigan, June 1975, Chapter 3.
4. D. Deirmendjian, "Scattering and Polarization Properties of Water Clouds and Hazes in the Visible and Infrared," Applied Optics 3, 187-196 (1964).
5. D. Deirmendjian, Electromagnetic Scattering on Spherical Poly-dispersions, American Elsevier Publishing Co., Inc., New York, (1969).
6. G. M. Hale and M. R. Querry, "Optical Constants of Water in the 200-nm to 200- $\mu$ m Wavelength Region," Applied Optics 12, 555-563 (1973).
7. J. E. Hansen, "Radiative Transfer by Doubling Very Thin Layers," Astrophys. J. 155, 565-573 (1969).
8. J. E. Hansen, "Exact and Approximate Solutions for Multiple Scattering by Cloudy and Hazy Planetary Atmospheres," J. Atmos. Sci. 26, 478-487 (1969).
9. J. E. Hansen and J. B. Pollack, "Near-Infrared Scattering by Terrestrial Clouds," J. Atmos. Sci. 27, 265-281 (1970).
10. J. E. Hansen, "Multiple Scattering of Polarized Light in Planetary Atmospheres. Part I. The Doubling Method," J. Atmos. Sci. 28, 120-125 (1971).
11. J. E. Hansen, "Multiple Scattering of Polarized Light in Planetary Atmospheres. Part II. Sunlight Reflected by Terrestrial Water Clouds," J. Atmos. Sci. 28, 1400-1426 (1971).
12. E. Bauer, "The Scattering of Infrared Radiation from Clouds," Applied Optics 3, 197-202 (1964).

13. H. H. Blau, Jr. and R. P. Espinola, "Spectral Properties of Clouds from  $2.5\mu$  to  $3.5\mu$ ," Applied Optics 10, 1897-1901 (1968).
14. R. P. Espinola, Spatial and Spectral Properties of Cloud Backgrounds from 2.65 to 2.95 Microns, Rpt. No. 70505F, A. D. Little, Inc., Cambridge, Massachusetts, January 1970.
15. W. M. Irvine, "Multiple Scattering by Large Particles. II. Optically Thick Layers," Astrophys. J. 152, 823-834 (1968).
16. D. Adamson, The Role of Multiple Scattering in One-Dimensional Radiative Transfer, NASA TN D-8084, National Aeronautics and Space Administration, Langley Research Center, Hampton, Virginia, December 1975.
17. R. E. Turner, "Atmospheric Effects in Remote Sensing," from Remote Sensing of Earth Resources, Vol. II, University of Tennessee, Knoxville, Tennessee (1974).
18. H. Rose, D. Anding, R. Kauth and J. Walker, Handbook of Albedo and Thermal Earthshine, ERIM 190201-1-T, Environmental Research Institute of Michigan, Ann Arbor, Michigan (June 1973).
19. L. M. Romanova, "The Solution of the Radiation-Transfer Equation for the Case When the Indicatrix of Scattering Greatly Differs from the Spherical One. I.," Optics and Spectroscopy 13, 238-241 (1962).
20. L. M. Romanova, "Solution to the Radiative Transfer Equation for the Case of a Highly Nonspherical Scattering Index. II.," Optics and Spectroscopy 13, 463-466 (1962).
21. L. M. Romanova, "Radiation Field in Plane Layers of a Turbid Medium with Highly Anisotropic Scattering," Optics and Spectroscopy 14, 135-138 (1963).
22. G. E. Hunt, "A Review of Computational Techniques for Analyzing the Transfer of Radiation through a Model Cloudy Atmosphere," J. Quant. Spectrosc. Radiat. Transfer 11, 655-690 (1971).
23. J. F. Potter, "The Delta Function Approximation in Radiative Transfer Theory," J. Atmos. Sci. 27, 943-949 (1970).
24. Y. S. Chou, "Approximate Method for Radiative Transfer in Scattering Absorbing Plane Parallel Media," Applied Optics 17, 364-373 (1978).

### THE IVAN A. GETTING LABORATORIES

The Laboratory Operations of The Aerospace Corporation is conducting experimental and theoretical investigations necessary for the evaluation and application of scientific advances to new military concepts and systems. Versatility and flexibility have been developed to a high degree by the laboratory personnel in dealing with the many problems encountered in the nation's rapidly developing space and missile systems. Expertise in the latest scientific developments is vital to the accomplishment of tasks related to these problems. The laboratories that contribute to this research are:

Aerophysics Laboratory: Launch and reentry aerodynamics, heat transfer, reentry physics, chemical kinetics, structural mechanics, flight dynamics, atmospheric pollution, and high-power gas lasers.

Chemistry and Physics Laboratory: Atmospheric reactions and atmospheric optics, chemical reactions in polluted atmospheres, chemical reactions of excited species in rocket plumes, chemical thermodynamics, plasma and laser-induced reactions, laser chemistry, propulsion chemistry, space vacuum and radiation effects on materials, lubrication and surface phenomena, photo-sensitive materials and sensors, high precision laser ranging, and the application of physics and chemistry to problems of law enforcement and biomedicine.

Electronics Research Laboratory: Electromagnetic theory, devices, and propagation phenomena, including plasma electromagnetics; quantum electronics, lasers, and electro-optics; communication sciences, applied electronics, semi-conducting, superconducting, and crystal device physics, optical and acoustical imaging; atmospheric pollution; millimeter wave and far-infrared technology.

Materials Sciences Laboratory: Development of new materials; metal matrix composites and new forms of carbon; test and evaluation of graphite and ceramics in reentry; spacecraft materials and electronic components in nuclear weapons environment; application of fracture mechanics to stress corrosion and fatigue-induced fractures in structural metals.

Space Sciences Laboratory: Atmospheric and ionospheric physics, radiation from the atmosphere, density and composition of the atmosphere, aurorae and airglow; magnetospheric physics, cosmic rays, generation and propagation of plasma waves in the magnetosphere; solar physics, studies of solar magnetic fields; space astronomy, x-ray astronomy; the effects of nuclear explosions, magnetic storms, and solar activity on the earth's atmosphere, ionosphere, and magnetosphere; the effects of optical, electromagnetic, and particulate radiations in space on space systems.

THE AEROSPACE CORPORATION  
El Segundo, California